

## EFFECTS OF Mg AND Cu CONTENT ON QUENCH SENSITIVITY OF Al–Si–Mg ALLOY

Sujoy K. Chaudhury

Indus University, Ahmedabad, Gujarat, India

Diran Apelian

Metal Processing Institute, Worcester Polytechnic Institute,  
100 Institute Road, Worcester, MA 01609, USA

Copyright © 2016 American Foundry Society  
DOI 10.1007/s40962-016-0020-z

### Abstract

*Effects of Mg and Cu content on quench sensitivity of Al–Si–Mg-based cast alloys were investigated. Jominy end-quench test was performed to evaluate the quench sensitivity of Al–Si–Mg and Al–Si–Mg–Cu-based alloys. It was observed that the quench sensitivity of Al–Si–Mg alloy rises with the increase in Mg content. In general, quench factor values rise with the increase in distance away from the chill end of Jominy end-quench test bar. This is because the precipitation rate of strengthening particles increases with the increase in the concentration of quenched-in vacancy. The concentration of quenched-in vacancy declines with the decrease in cooling rate away from the chill end of test bar. The maximum quench factor value of Al–Si–0.57Mg alloy is 144.8, whereas those of Al–Si–0.35Mg and Al–Si–0.45Mg alloys are 38.5 and 34.8, respectively. This is in contrast to the quench factor values obtained in Al–Si–Mg alloy*

*containing 0.8 %Cu. Results show that an addition of 0.8 % Cu to Al–Si–Mg alloy significantly reduces the quench sensitivity of the alloy. Quench factor values of Al–Si–Mg–0.8Cu alloy are in the range of 1–16. No significant reduction in the quench factor is observed on addition of 0.23 and 0.50 wt% of Cu to Al–Si–Mg alloy. Simulation results show that Guinier–Preston (GP) zones form in the Al matrix when the amount of Cu in the Al–Si–Mg alloy exceeds 0.57 wt% during the natural aging subsequent to quenching. These GP zones are well-known heterogeneous sites for nucleation of precipitates and are responsible for reducing quench sensitivity of the Al–Si–Mg–0.8Cu alloy.*

**Keywords:** Jominy quench, heat treatment, Al–Si–Mg (Cu) alloy, quench sensitivity, magnesium, copper

### Introduction

The Al–Si–Mg-based cast alloys are widely used in the automotive industry due to their good castability, good fatigue strength, and high strength to weight ratio.<sup>1</sup> In Al–Si–Mg alloys, Mg combines with Si to form various metastable phases ( $Mg_xSi_y$ ) and stable  $Mg_2Si$  phase during aging treatment. Precipitation of semi-coherent  $Mg_xSi_y$  metastable phases in Al–Mg–Si alloys makes them heat treatable.<sup>2,3</sup> In general, these alloys are heat-treated to T6 temper. The T6 temper comprises of solution heat treatment at a temperature around 540 °C (1004 °F), quenching, and artificial aging at a temperature between 150 and 200 °C (302–392 °F).<sup>4,5</sup> Solution heat treatment increases ductility and strength of the cast alloy. The increase in ductility is due to the spheroidization of eutectic Si

particles, while the increase in strength is due to solid solution strengthening of Al matrix. The quenching process helps to retain solutes and vacancy complexes in the Al matrix. Vacancies are point defect with unoccupied lattice sites. The distribution of such defects in as-quenched state is in the form of complexes. The retention of vacancy complexes is very important, as it plays a key role on the kinetics of precipitation of phase(s) during subsequent aging treatment.

It is reported that the aging kinetics depends on several factors.<sup>6–9</sup> Among them, the most important factors are: (1) vacancy concentration and (2) Guinier–Preston (GP) zones formation. A GP zone is a solute-enriched region in the alloy, and its size is in the order of few nanometers. In Al–Si–Mg alloy, GP zones constitute of Mg and Si as solute

atoms, whereas in Al–Si–Mg–Cu alloy, GP zones constitute of Mg, Si, and Cu as solute atoms. In addition, aging kinetics also depends on some extrinsic parameters such as aging temperature and heating rate, and intrinsic parameters such as diffusivity and activation energy. It is reported that high vacancy concentration in Al matrix increases diffusivity of alloying elements and therefore increases precipitation rate.<sup>6</sup> In general, vacancy concentration in Al matrix is high when it is quenched at higher cooling rate.

In most commercial applications, water is used as the quenchant because of the following reasons: high cooling rates, no environmental issues, and low operating cost. However, the use of water as a quenchant often causes distortion and generates undesirable residual stresses in complicated shaped parts that often limit water's usage to those applications that are less sensitive to structural deformation. Therefore, there is great impetus to search for an alternate quenchant that has the potential to overcome problems such as structural deformation and residual stresses, which is commonly observed in water-quenched components. The ideal situation would be elimination of the quenching step without compromising strength and ductility.

It is widely reported<sup>10</sup> that Al–Si–Mg-based cast alloys are highly sensitive to cooling rate during the quenching process. In other words, mechanical properties such as hardness and tensile strength decrease significantly on reducing cooling rates during quenching. These alloys are generally quenched in water to achieve desired combination of strength and ductility. This limits their applicability only to situations with less stringent structural integrity requirements, and where residual stress is not of paramount importance. Therefore, there is a need to redesign alloy to reduce its quench sensitivity. In this study, effects of Mg and Cu content on quench sensitivity of Al–Si-based alloys were investigated. The objective of this study is to tailor the chemical composition of Al–Si–Mg-based cast alloys to make them less quench sensitive and determine the optimum composition to achieve the same.

## Experimental Methods

### Casting of Test Bar

Alloys, namely Al–Si–Mg and Al–Si–Mg–Cu, with varying amounts of Mg and Cu were cast in a permanent mold. The alloy was prepared by melting Al in an induction furnace, and the calculated amount of master alloys, namely Al–Si, Al–Mg, Al–Sr, and Al–Cu, was added to the melt. The alloy was cast in the form of cylindrical bars in a permanent mold preheated to 425 °C (797 °F). Prior to casting, the melt was degassed by passing nitrogen through the melt using a rotary degasser. The pouring temperature of the melt was 800 °C (1472 °F). The dimension of the cylindrical bar was 25 mm in diameter and 230 mm in

height. For Jominy end-quench test, each bar was cut into two halves. Melt chemistry was routinely monitored using an optical emission spectrometer during the casting process. Alloy chemistries reported are an average of at least five measurements.

### Heat Treatment and Jominy End-Quench Test

The quench sensitivity study was carried out following the Jominy end-quench test.<sup>11</sup> The Jominy quench test basically consists of cooling cast bars from one end by a water quenching device suitable to provide a vertical stream of water. The water pressure was adjusted so that the stream of water rises to a free height of about 64 mm above the orifice without the specimen in position. Then, the heated specimen was placed so that its bottom face was 12 mm above the orifice. The time between removal of specimen from the furnace and beginning of quench was less than 5 s. A still-air condition was maintained around the specimen. Jominy end-quench set up is shown in Figure 1. Detailed description of Jominy end-quench test is given in ASTM designation A255-02. Alloys were solutionized at 538 °C (1000 °F) for 6 h in a tubular furnace prior to the Jominy end-quench test. Subsequently, after the Jominy end-quench test, alloys were aged at 175 °C (347 °F) for 5 h. The incubation time between solution heat treatment and aging was 48 h.

### Thermal Analysis

The cooling profile of the test bar was monitored using K-type thermocouples placed at different locations in the test bar. Holes were drilled on the test bar, and thermocouples were inserted in it. Care was taken to ensure that

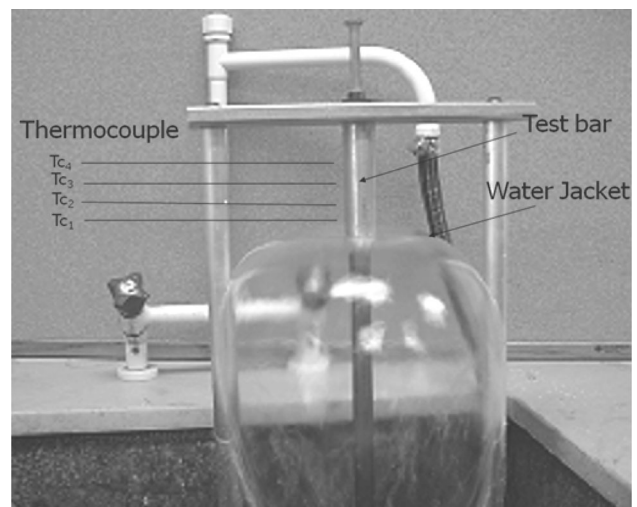


**Figure 1. Jominy quench setup. The sample was connected to four thermocouples at four locations ( $T_{c1}$ ,  $T_{c2}$ ,  $T_{c3}$ , and  $T_{c4}$  shown in the figure).**

during the Jominy end-quench test water did not penetrate into the hole and the thermocouple was rigidly held in the test bar. Data was acquired at a frequency of 10 readings per second using a data acquisition system.

## Microstructural Characterization

Microstructural characterization of T6 tempered alloys was carried out using a scanning electron microscope (SEM). Phases were identified by energy-dispersive X-ray analysis. Samples for microscopy were prepared by grinding with emery paper and electropolishing at 35 V for 20 s. The composition of the electrolyte (in volume percent) was 60 pct ethyl alcohol, 20 pct perchloric acid, and 20 pct ethylene glycol.

## Hardness Measurement

Rockwell hardness ( $R_B$ ) was measured at different locations on the test bar. The surface of the cylindrical bar was flattened before the test. Four measurements were taken at each distance away from the chill end, and the average value is reported.

## Results and Discussion

### Thermal Analysis

Cooling curves and their first derivatives obtained from Jominy quench test of a cylindrical bar at different locations away from the chill end are shown in Figure 2a, b, respectively. As expected, the cooling rate decreases with an increase in the distance away from the quench end. The chill end undergoes maximum cooling rate. The variation of cooling rate with temperature typically exhibits an inverse “C” curve, which implies that the cooling rate increases in the beginning of the quench and is followed by a gradual decrease at a later stage. The maximum cooling rate at a distance of 3 mm away from the chill end is 107 °C/s (192.6 °F/s).

### Effect of Mg Content on Quench Sensitivity of Al–Si–Mg Alloy

The chemical composition of various Al–Si–Mg alloys is given in Table 1. The Mg content in the Al–Si–Mg alloy was varied to 0.35, 0.45, and 0.56 wt%, respectively. The amount of Si in these alloys is around 7 wt%. In addition, alloys contain other alloying elements such as Sr as modifier, Ti as grain refiner, and Fe as an impurity element. The amount of Ti is considered as quite high in these alloys. This level of Ti has been observed to delay aging kinetics in 356/357 alloys.<sup>15</sup>

Results of the Jominy end-quench test on Al–Si–Mg alloys containing different amounts of Mg are shown in Figure 3a, b. Figure 3a shows the variation in hardness with distance away from the chill end of the Jominy quench test bar, and their respective variations in quench factor are shown in Figure 3b. As expected, hardness decreases with an increase in the distance away from the chill end and consequently results in high quench factor values at locations away from the chill end. Similar observations were made by Pedersen et al.<sup>10</sup>, where they reported that after solution heat treatment tensile strength of the Al–Si–Mg (A356) alloy was less at low quench rate. The quench factor ( $\tau$ ) is calculated for any location on the Jominy end-quench bar from hardness measurements using Eqn. 1:<sup>12</sup>

$$\tau = \frac{1}{K_n} \ln \left( \frac{H_{VN}}{H_{max}} \right) \quad \text{Eqn. 1}$$

where  $\tau$  is the quench factor,  $H_{VN}$  is the hardness at a specific location on the Jominy end-quench bar,  $H_{max}$  is the maximum hardness,  $K_n$  is taken to be the value of  $\ln(0.995)$ .

Highest quench factor values for alloy containing 0.35, 0.45, and 0.57 wt% of Mg are 38.5, 34.8, and 144.8, respectively. No significant difference is observed between quench factor values of alloy containing 0.35 and 0.45 wt% of Mg. However, the alloy containing 0.57 wt% of Mg shows very high quench factor values as compared to those containing 0.35 and 0.45 wt% of Mg. This implies that high Mg content (0.57 wt%) in the Al–Si–Mg alloy makes it more sensitive to cooling rate.

As expected, hardness rises with increasing amounts of Mg in Al–Si–Mg alloys. This is because the amount of strengthening phases such as metastable  $\beta'$ ,  $\beta''$ , and  $B'$  and stable  $Mg_2Si$  precipitates formed in the Al–Si–Mg alloy is greater in alloys with higher Mg content. Thermodynamic simulation results using JMatPro™ software show that the amount of  $Mg_2Si$  phase formed in the Al–7Si–xMg alloy containing 0.3, 0.45, and 0.57 wt% of Mg are 0.55, 0.71, and 0.88 wt%, respectively. It is well known that metastable  $\beta'$ ,  $\beta''$ , and  $B'$  and stable  $Mg_2Si$  precipitates in Al–Si–Mg alloys cause precipitation strengthening. Simulation results of Al–7Si–xMg alloy that was solutionized at 540 °C (1004 °F), quenched, and aged at 175 °C (347 °F) for 5 and 28 h are given in Table 2. As is evident from data in Table 2, the amount of  $Mg_2Si$  phase formed in the Al–7Si–xMg alloy after heat treatment is greater in the alloy with high Mg content. Strength of the alloy increases with an increase in the amount of precipitate formed during aging in the matrix. In general, aging of Al–7Si–xMg alloy results in the formation of metastable phases such as  $\beta'$ ,  $\beta''$ , and  $B'$  in the early stage of aging and  $Mg_2Si$  as stable phase during later stage of aging. It has been reported that peak hardness during aging of Al–7Si–xMg alloy is achieved due to the precipitation of semi-coherent metastable phases such as  $\beta'$ ,  $\beta''$ , and  $B'$ .<sup>14</sup> Therefore, it is

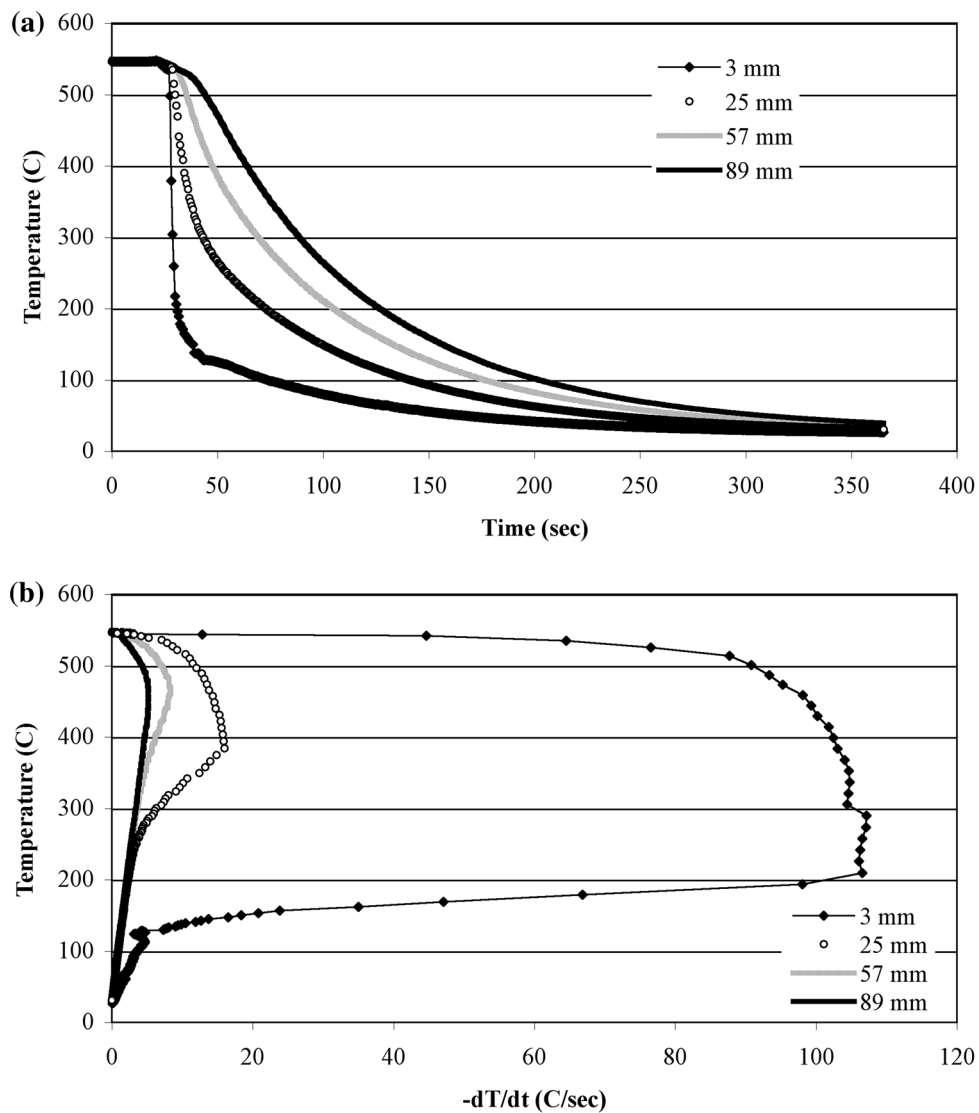


**Figure 2. (a) Cooling curves and their (b) first derivatives obtained from a Jominy end-quench test. Distance shown in the legend of the figure (i.e., 3, 25, 57, and 89 mm) is the distance away from the chill end of the bar.**

**Table 1. Chemical Composition of Al-Si-Mg Alloys (Varying Mg Content)**

Alloy	Si	Fe	Mg	Ti	Sr	Al
A356	7.26	0.12	0.35	0.17	0.009	Balance
	7.06	0.083	0.45	0.177	0.011	Balance
A357	6.95	0.097	0.56	0.172	0.013	Balance

expected that the Al matrix will consist of combination of stable  $Mg_2Si$  phase and metastable phases such as  $\beta'$ ,  $\beta''$ , and  $B'$  after aging for 5 h at 175 °C (347 °F).

### Effect of Cu Content on Quench Sensitivity of Al-Si-Mg Alloy

Chemical compositions of Al-Si-Mg-Cu alloy containing different levels of Cu and Mg are given in Table 3. Results from hardness test on heat-treated A356 (Al-Si-Mg) alloy and those containing 0.2, 0.5, and 0.8 wt% of Cu are shown in Figure 4a, b. As expected, the average hardness of the alloy rises with increasing Cu content. In general, the hardness of the alloy with Cu content less than 0.8 wt% decreases with the increase in distance away from the chill end of the Jominy quench bar. In case of the alloy with no Cu (i.e., A356 alloy), the difference of hardness between

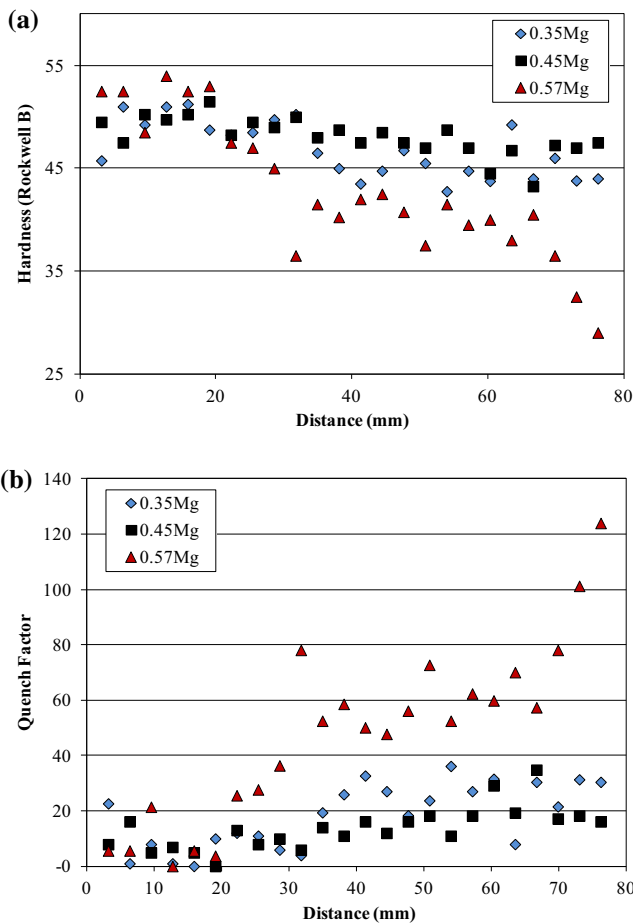


**Figure 3.** Variations in (a) hardness and (b) quench factor with distance away from the chill end of Jominy quenched bars of Al-Si-Mg alloys. Each alloy was aged at 175 °C (347 °F) for 5 h subsequent to Jominy end-quench test.

**Table 2.** Amount of Mg<sub>2</sub>Si Formed After Heat Treatment [i.e., Solutionized at 540 °C (1004 °F), Quenched, and Aged at 175 °C (347 °F) for 5 and 29 h] in Al-7Si-xMg Alloy

Alloy	Atomic % of Mg <sub>2</sub> Si	
	Aging time = 4.9 h	Aging time = 27.9 h
Al-7Si-0.35Mg	0.13	0.45
Al-7Si-0.45Mg	0.18	0.59
Al-7Si-0.56Mg	0.22	0.72

the chill end and those away from the chill end is significantly large. Similar observations are made on alloys containing 0.2 and 0.5 wt% of Cu. On the contrary, the decrease in hardness of A356-0.8Cu alloy moving away from the chill end is marginal. This is reflected on relatively lower quench factor values of A356-0.8Cu alloy as compared to other alloys, namely A356, A356-0.2Cu, and A356-0.5Cu. Variations in quench factor for Al-Si-Mg alloys containing different levels of Cu are shown in

**Table 3.** Chemical Compositions of Al-Si-Mg Alloys (Varying Cu Content)

Si	Fe	Cu	Mg	Ti	Sr	Al
7.26	0.12	0.011	0.34	0.099	0.009	Balance
7.13	0.123	0.23	0.34	0.099	0.009	Balance
6.79	0.12	0.50	0.33	0.1	0.008	Balance
7.0	0.118	0.83	0.35	0.155	0.011	Balance
7.4	0.094	0.83	0.45	0.19	0.014	Balance

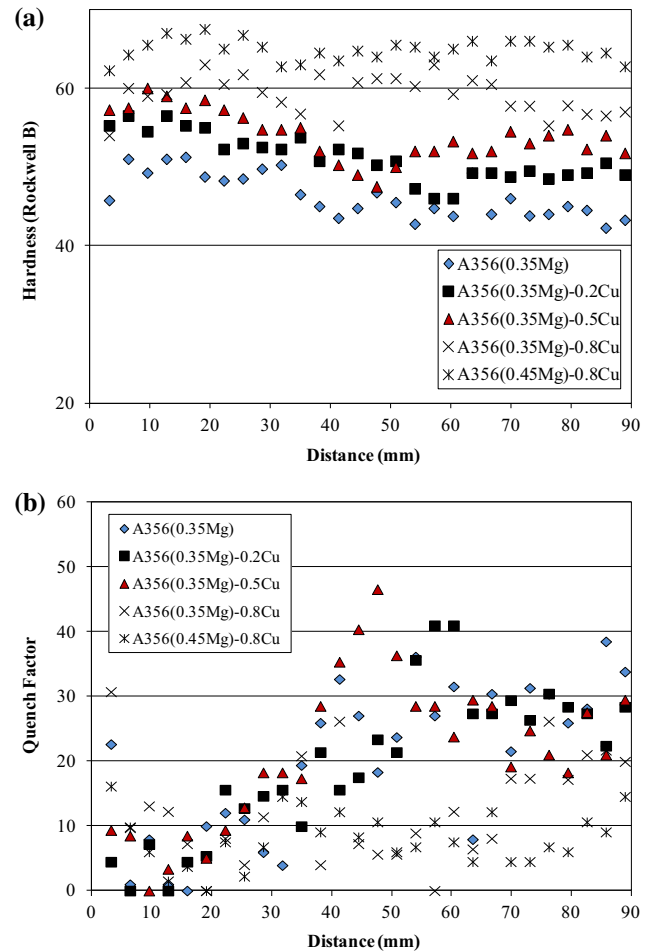


**Figure 4.** Variations in (a) hardness and (b) quench factor with distance away from the chill end of Jominy quenched bars of Al-Si-Mg-Cu alloys.

Figure 4b. Quench factor values at distances between 25 and 100 mm away from the chill end of Al-0.45Mg-0.8Cu alloy test bar are lowest and they varied in the range of 10-16, whereas quench factor values of A356 alloy varied in the range of 30-40.

It is clear that Al-Si-Mg-0.8Cu alloys (containing 0.35 and 0.45 wt% of Mg) are least quench sensitive as compared to A356, A356-0.2Cu, and A356-0.5Cu alloys. No significant difference was observed between quench factor values of Al-Si-Mg alloy and those containing 0.2 and

0.5 wt % of Cu. The reduction in quench sensitivity of Al-Si-Mg-0.8Cu alloy is attributed to the uniform precipitation of Q phase, which is the primary strengthening phase in this alloy. The Q phase nucleates on GP zones that formed during the natural aging stage. Quench sensitivity results are explained from simulated TTT diagrams and microstructural examination discussed below in Sects. “Simulation of time-temperature transformation (TTT) diagrams” and “Microstructural observations.”

### Simulation of Time-Temperature Transformation (TTT) Diagrams

To understand the role of Cu on quench sensitivity of the Al-Si-Mg (Cu) alloy, TTT diagrams were simulated using

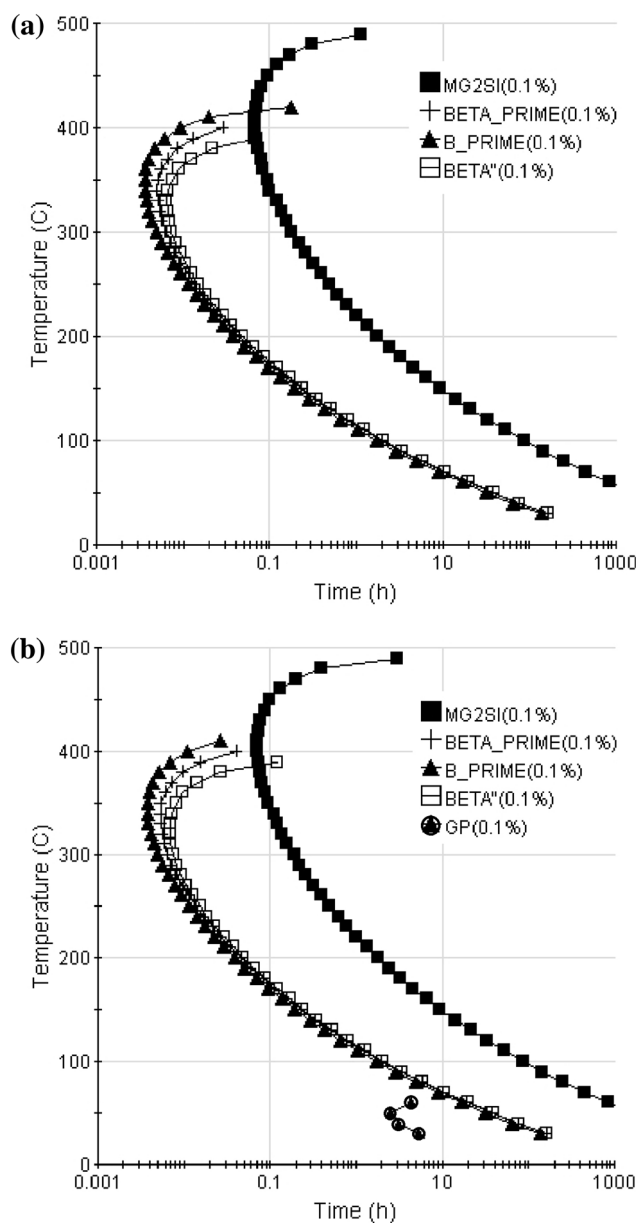


Figure 5. TTT diagram of (a) A356 (Al-7Si-0.2Fe-0.35Mg-0.15Ti-0.01Sr) alloy, (b) A356-0.8Cu alloy.

JMatPro<sup>®</sup> software. Saunders et al.<sup>13</sup> have reported good accuracy to predict TTT diagrams of some generalized steels using the software. However, reports on experimental validation of such calculations are limited to steels, and not much information is available on Al alloys. The TTT diagrams of A356 and A356-0.8Cu alloy are shown in Figure 5a, b, respectively. One clear difference between them is the presence of GP zones in the TTT diagram of A356-0.8Cu alloy, while it is absent in the TTT diagram of A356 alloy (Figure 5a). These GP zones are well-known heterogeneous sites for nucleation of precipitates during aging of the alloy. The reduced quench sensitivity of A356-0.8Cu alloy as compared to those of A356, A356-0.2Cu, and A356-0.5Cu alloys is attributed to the formation of GP zones in the former (i.e., A356-0.8Cu), whereas no GP zones form in latter cases (i.e., A356, A356-0.2Cu, and A356-0.5Cu) during the incubation time subsequent to quenching after solution heat treatment. Simulation results have shown that GP zones form only when the Cu content in the A356 alloy is greater than 0.57 % by weight. The kinetics of GP zone formation at 50 °C (122 °F) and 25 °C (77 °F) in the A356-0.8Cu alloy are shown in Figure 6a, b, respectively. In both cases, the selected solutionizing temperature was 500 °C (932 °F). Simulation results show that the kinetics of GP zone formation is faster at 50 °C vis-à-vis at 25 °C. The amount of GP zones formed at 50 °C (122 °F) and at 25 °C (77 °F) are 0.6 and 0.38 at.%, respectively. Times required for the formation of 0.6 at.% of GP zones at 50 °C (122 °F) and 0.38 at.% of GP zones at 25 °C (77 °F) are 2 and 20 h, respectively. Therefore, it is recommended that the alloy (A356-0.8Cu) should be naturally aged for minimum of 20 h at room temperature [i.e., 25 °C (77 °F)] or pre-aged for 2 h at 50 °C (122 °F) to benefit from the GP zone formation. The GP zones help to enhance overall aging

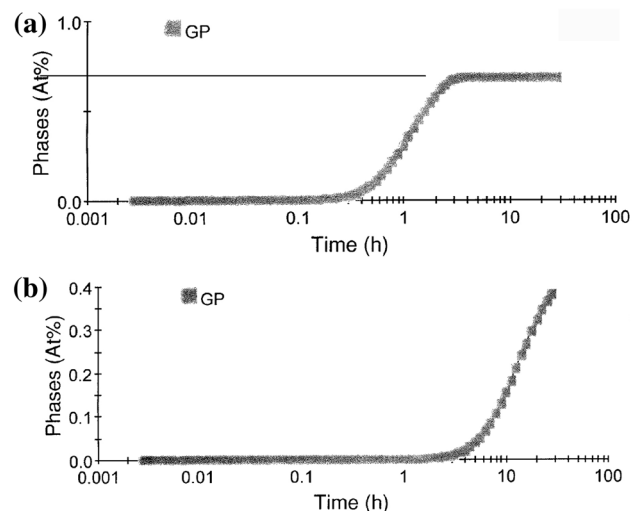
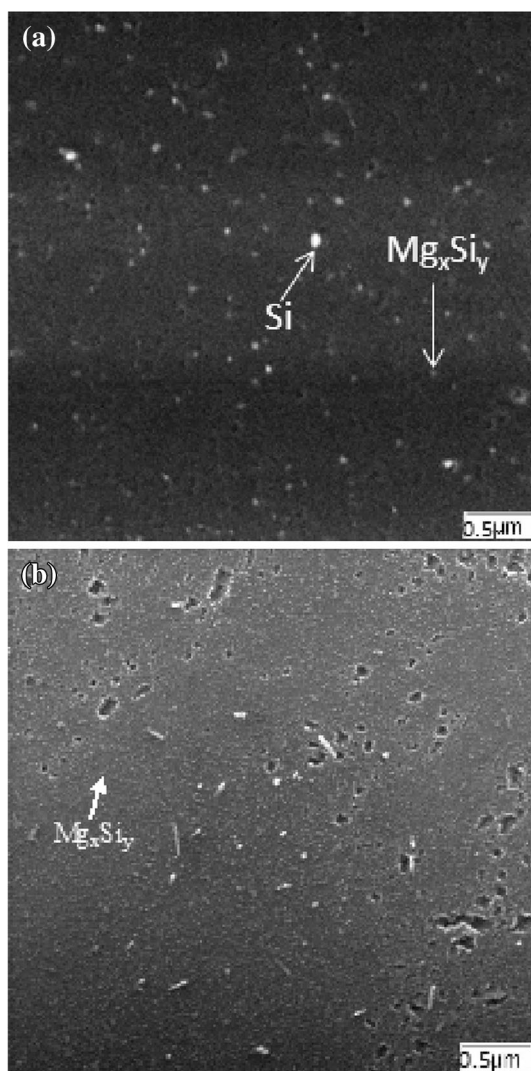


Figure 6. Kinetics of GP zone formation at (a) 50 °C and (b) 25 °C holding temperatures. In both cases, the solutionizing temperature is 500 °C and the alloy is A356(0.35Mg)-0.8Cu.



**Figure 7. SEM micrographs of A356 alloy (T6) (a) Far away from the chill end (3.5'), and (b) Near the chill end (0.25') of the Jominy quenched test bars. Subsequent to Jominy end-quench test, the sample was aged at 175 °C for 5 h.**

kinetics of the alloy and consequently reduce the quench sensitivity of the alloy.

In addition to  $Mg_2Si$  as equilibrium phase, the simulation results show the presence of metastable phases such as  $\beta'$  (BETA\_PRIME) and  $\beta''$  (BETA''), and  $B'$  (B-PRIME). The stoichiometry and nomenclature of these metastable phases are reported by Edwards et al.<sup>16</sup> It is clearly evident from simulated results that metastable phases form in the initial stage of aging treatment (i.e., under aging and peak aging conditions) and equilibrium phase (i.e.,  $Mg_2Si$ ) forms at the later stage of aging treatment (i.e., overaging condition). The A356 alloy is hardened primarily by semi-coherent  $Mg_xSi_y$  metastable phases (such as metastable  $\beta'$ ,  $\beta''$ , and  $B'$ ).<sup>17</sup> The ratio of Mg:Si in these metastable phases is close to 1:1.

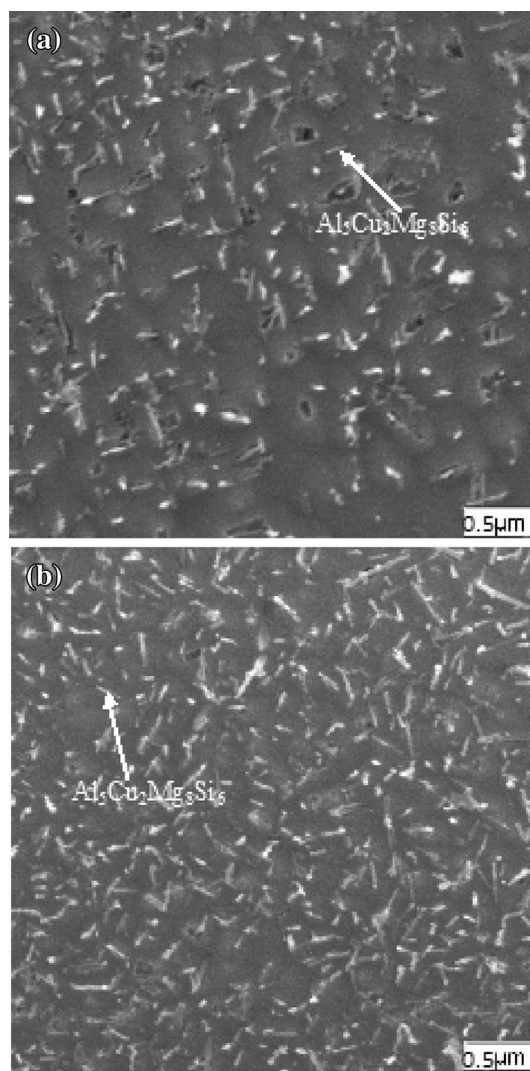


**Figure 8. SEM micrographs of A356-0.8Cu alloy (T6) (a) Far away from the chill end (3.5'), and (b) Near chill end (0.25') of the Jominy quenched test bar. Subsequent to Jominy end-quench test, the sample was aged at 175 °C for 5 h.**

### Microstructural Observations

The effect of cooling rate on microstructure of A356 and A356-0.8Cu alloys is shown in Figures 7a, b and 8a, b, respectively. The near-end refers to the high cooling rate region, while the far-end refers to the low cooling rate region. In case of A356 alloy, the precipitating phase consists of combination of  $Mg_xSi_y$  as metastable phases and thermodynamically stable  $Mg_2Si$  phase,<sup>14</sup> whereas in the case of A356-0.8Cu alloy, the precipitating phase is  $Al_5Cu_2Mg_8Si_6$ . Microstructural observations clearly reveal that in the case of A356 alloy, the number density of Mg-Si precipitates in the near-end region is greater than far away region from the chill. This accounts for the high hardness in the near chill end as compared to those far

away from the chill end. On the contrary, the number density of  $\text{Al}_5\text{Cu}_2\text{Mg}_8\text{Si}_6$  precipitates in A356–0.8Cu alloy does not vary significantly with distances away from the chill end. The uniform distribution of precipitates in A356–0.8Cu alloy resulted in reduced values of quench factor as discussed above, and hence, the alloy is less quench sensitive.

## Conclusions

- Quench sensitivity of Al–Si–Mg cast alloys depends on the amount of Mg. It is observed that quench sensitivity of Al–Si–Mg alloy increases with the increase in the amount of Mg. The maximum quench factor ( $\tau$ ) value observed in Al–Si–0.57Mg alloy is 145, which is significantly high as compared to Al–Si–0.35Mg ( $\tau = 38$ ) and Al–Si–0.45Mg ( $\tau = 35$ ) alloys.
- Addition of 0.8 wt% of Cu to A356 significantly lowers its quench sensitivity. The maximum quench factor value of Al–Si–0.45Mg–0.8Cu alloy is 16, which is the least value among all other alloys. This shows that Al–Si–0.45Mg–0.8Cu alloy is the least quench sensitive.
- The precipitation rate of metastable  $\text{Mg}_x\text{Si}_y$  and thermodynamically stable  $\text{Mg}_2\text{Si}$  precipitates in A356 alloy decreases with decreasing quench rates. On the contrary, the precipitation rate of  $\text{Al}_5\text{Cu}_2\text{Mg}_8\text{Si}_6$  in Al–Si–Mg–Cu alloy is relatively independent of cooling rate during quenching after solution heat treatment.
- Simulation results show that the addition of Cu in excess of 0.57 wt% to Al–Si–Mg alloy forms GP zones; these GP zones are heterogeneous sites for nucleation of precipitates and reduce the quench sensitivity of the alloy.
- Simulation results show that it takes about 20 h for the GP zones to form at room temperature [i.e., 25 °C (77 °F)] in Al–Si–Mg–0.8Cu alloy during incubation time after solution heat treatment. Therefore, it is recommended that the alloy containing 0.8 wt% of Cu should be naturally aged for a minimum period of 20 h prior to aging to increase the aging kinetics of the alloy.

## Acknowledgments

Authors thank the corporate members of the Advanced Casting Research Center of the Metal Processing Institute for their support of this work.

## REFERENCES

1. C.H. Caceres, C.J. Davidson, J.R. Griffiths, L.M. Hogan, Q.G. Wang, *Mater. Forum* **21**, 27–43 (1997)
2. D. Apelian, S. Shivkumar, G. Sigworth, *AFS Trans.* **89–137**, 727–741 (1989)
3. Q.G. Wang, C.J. Davidson, *J. Mater. Sci.* **36**(3), 739–750 (2004)
4. S.K. Chaudhury, D. Apelian, *J. Mater. Sci.* **41**(14), 4684–4690 (2006)
5. S.K. Chaudhury, L. Wang, D. Apelian, *AFS Trans.* **112**, 1–16 (2004)
6. J.M. Silcock, *Philos. Mag.* **4**, 1187–1193 (1959)
7. C. Garcia-Cordovilla, E. Louis, *Metall. Mater. Trans. A* **15A**, 389–391 (1984)
8. T. Chen, G. Phen, J.C. Huang, *Metall. Mater. Trans. A* **27A**, 2923–2933 (1996)
9. K. Hirose, S. Hirosawa, T. Sato, *Mater. Sci. Forum* **396–402**, 795–800 (2002)
10. L. Pedersen, L. Arneberg, *Metall. Mater. Trans. A* **32A**, 525–532 (2001)
11. J. Marrow, *Ind. Heat.* **68**(9), 57–60 (2001)
12. S. Ma, M.D. Maniruzzaman, R.D. Sisson Jr., *ASM heat treating society conference and exposition*, Pittsburgh, PA, USA, 26–28 Sept 2005
13. N. Saunders, Z. Guo, X. Li, A.P. Miodownik, J.-P. Schille, *J. Metals* **55**, 60–65 (2003)
14. R.N. Lumley, I.J. Polmear, P.R. Curtis, *Rapid heat treatment of aluminum high pressure diecastings*. *Metall. Mater. Trans. A* **40A**, 1716–1726 (2009)
15. M.S. Misra, K.J. Oswalt, *Aging characteristics of titanium-refined A356 and A357 aluminum castings*. *AFS Trans.* **90**, 1–10 (1982)
16. G.A. Edwards, K. Stiller, G.L. Dunlop, M.J. Cooper, *The precipitation sequence in Al–Mg–Si alloys*. *Acta Mater.* **46**, 3893–3904 (1998)
17. N. Saunders, *The modelling of stable and metastable phase formation in multi-component Al-alloys*. *Mater. Forum* **28**, 96–106 (2004)



## Technical Review & Discussion

### Effects of Mg and Cu Content on Quench Sensitivity of Al–Si–Mg Alloy

Sujoy K. Chaudhury; Indus University, Ahmedabad, Gujarat, India

Diran Apelian; Worcester Polytechnic Institute, Metal Processing Institute, Worcester, MA, USA

**Reviewer:** Regarding precipitation hardening; while it is generally correct to refer to the Mg–Si precipitation hardening system as Mg<sub>2</sub>Si based, the maximum hardness is generally achieved in the semi-coherent Beta prime and Beta double prime region. By the time the end-stage incoherent Mg<sub>2</sub>Si particles reach dominance you are in the over-aged and softened region of the aging curve. So we must be careful referring to the precipitates you see in the Al–Si–Mg alloys as all being Mg<sub>2</sub>Si in the T6 temper.

**Authors:** Agreed. The precipitation sequence is discussed in the revised manuscript. The reviewer is right that metastable phases such as beta prime, beta double prime, B-prime contribute significantly to peak hardening condition. After 5 hours of aging, it is expected that the matrix will consist of combination of stable and metastable phases.

**Reviewer:** What is the difference between Beta, B\_Prime and Beta\_Prime?

**Authors:** Beta, B\_Prime and Beta\_prime are metastable phases formed during the initial stage of precipitation with Mg:Si ratio close to 1:1 and the nomenclature was used by Edwards et al. This has been discussed and referenced in greater detail in the revised paper.

**Reviewer:** You state that GP zones do not form in A356 alloy. My understanding is that there is a sequence of reactions during aging. Precipitation starts with the formation of spherical GP zones from the supersaturated solid solution (Al<sub>ss</sub>). These quickly elongate into the direction of the aluminum matrix and assume a needle shape. They grow to become rods, and eventually platelets. Peak hardness is just before platelets form. β' is a semi-coherent phase. The final, equilibrium β phase (Mg<sub>2</sub>Si) nucleates on β'.

**Authors:** The simulation result predicted that GP zones do not form during the natural aging of A356 alloy subsequent to quenching after solution heat treatment. It is a generally accepted theory that GP zones form in A356 alloy followed by precipitation of metastable at the early stage and stable precipitates at the later stage (i.e. overaging). However, the simulation result from JMatPro showed that GP zones do not form in A356 alloy irrespective of holding time after quenching from solutionizing temperature. Similar observations have been reported by Saunderson and referenced in the revised paper. I agree with reviewer's comment on the evolution metastable and stable precipitates and the same is added in the revised manuscript.